Isothermal and anisothermal decomposition of Carbon fibres polyphenylene sulfide composites for fire behavior analysis

Yann Carpier, Benoît Vieille, Nicolas Delpouve, Eric Dargent

Isothermal and anisothermal decomposition of Carbon fibres polyphenylene sulfide composites for fire behavior analysis

Carpier Y, Vieille B*, Delpouve N, Dargent E

Normandie Univ, UNIROUEN Normandie, INSA Rouen, CNRS, Groupe de Physique des Matériaux

76800 ROUEN, France

*Correspondence to: benoit.vieille@insa-rouen.fr

Abstract

This work was aimed at studying the influence of severe temperature conditions representative of fire conditions on thermal decomposition of both plain PPS thermoplastic resin and C/PPS laminates. The investigations on the relationship between local temperature resulting from the local balance energy exchange, the local atmosphere and the mass losses are essential in understanding the influence of fire on polymers and polymer matrix composites. This involves first identifying the thermal decomposition phenomena involved by means of thermogravimetric analyses conducted in both isothermal and anisothermal testing conditions, as well as under inert and oxidizing atmospheres. As far the heating conditions (isothermal and anisothermal) are concerned, an increase in the testing temperature leads to increasing decomposition rates, as expected. In anisothermal conditions oxidation starts before the end of pyrolysis, whereas, pyrolysis is complete before oxidation in isothermal conditions. Regarding the influence of fibers on the thermal decomposition mechanisms in PPS-based composites, the cross-linking may be promoted by the presence of fibers resulting in delaying the onset of pyrolysis under oxidizing atmosphere. Such cross-linking is not significant enough to observe such a delay under air. Finally, MT-TGA tests under inert atmosphere seem to reveal three different mechanisms during pyrolysis in agreement with conclusions drawn in the literature on the same material: depolymerization, random chain scission and ultimately cyclisation (char formation).

Keywords: fire; thermal decomposition; thermoplastic; isothermal; anisothermal

1. Introduction

In aeronautics fire is one of the most critical conditions in service for materials. When plane parts consist of Polymer Matrix Composite (PMC) materials, the criticality is even higher because most PMCs usually cannot bear significant mechanical loading at temperature higher than 200-250°C. High-performance thermoplastic-based (TP) composites (e.g. PEEK, PPS, PEI…) are promising materials for structural applications in aeronautics as they are resistant to impact. They have a good damage tolerance as well as they have a very good retention of their mechanical properties under fire conditions. Among the most common PMCs used in load-bearing aircraft structures Carbon/epoxy (thermosetting) composites are flammable and readily decompose when exposed to heat and fire. In the literature most of the studies dealing with the fire behavior of composite materials focus on thermosetting-based composites [1] but very few on thermoplastic-based composites [2][3]. To better understand the changes in the thermal and mechanical behaviors of polymer-based composites under fire exposure the first step usually is to investigate the influence of thermal heat fluxes, hence temperature, resulting from a fire. Such heat fluxes lead to significant temperature differences within composite structures. From thermal analyses it is therefore possible to study the decomposition mechanisms as well as their kinetics under different testing conditions (heating rate, isothermal and anisothermal, inert or oxidizing atmosphere). The decomposition mechanisms are closely associated with the chemical nature of the polymer [4].

Figure 1 presents the characteristic behaviour of a thermoplastic material subjected to a heat flux on one side. The heat conduction within the material causes physical and chemical transformations. Through the thickness there are different transformations such as thermal degradation and thermal decomposition in a cross section called the "mesophase". When the material undergoes a thermal decomposition there are changes in the chemical composition and the structure of the material depending on the atmosphere (inert or oxidizing) in which the decomposition occurs (see Fig. 1). Pyrolysis of polymer matrix produces a liquid called tar and a non-condensable gas. Char is produced by repyrolysing the tar [5] and results from the thermal decomposition of organic resins and fibres. It is a highly porous material that can consist of

crystalline (i.e. graphitic) and/or amorphous regions [6]. Under oxidizing atmosphere decomposition gases can ignite and cause the material to ignite. All these chemical changes are accompanied by sudden changes in physico-chemical and mechanical properties [7].

In the mesophase gas bubbles form within a phase whose viscosity decreases with temperature. On the surface the bubbles burst and release combustible gases that may fuel the flame. If portions of material remain non-gasified, then they form viscous tars that accumulate on the surface. From a thermal point of view this thermal decomposition has many consequences. Indeed the chemical mechanisms of decomposition (pyrolysis, oxidation, inflammation) are accompanied by heat exchanges, which influence the energy balance: endothermic reaction for the first, exothermic for the other two. The resulting change in properties is also accompanied by a significant perturbation of heat exchanges within the material. The effective conductivity decreases through the thickness due to the formation of porosity but also on the exposed surface due to the change in material emissivity.

1.1 Thermal decomposition in PMCs

First of all polymers have diverse chemical compositions and structures, which involve various thermal decomposition mechanisms [8]: (i) depolymerization, (ii) random chain scission, (iii) chain stripping, (iv) cyclisation. Although the thermal decomposition of a polymer can theoretically be observed according to only one of these mechanisms, it is generally the combination of several of them as the temperature increases and results in the formation of many decomposition products. It can be considered complete when any solid residue is fully vaporized or gasified. Among the commonly used polymer materials for aeronautics applications epoxy resin is known for its poor fire resistance [1], phenolic resins are also widely used as thermal protection whereas fire-improved epoxy resins are sometimes considered as ablative protection for internal thermal insulation [9]. Compared to common thermosetting resins (phenolic and epoxy) used for high temperature conditions polyether-ether-ketone (PEEK) and PolyPhenylene Sulfide (PPS) thermoplastic resins known for their high-temperature stability proved to have higher thermal performance, particularly with a higher decomposition temperature [6]. In TP polymers, melting is a

general stage of char formation and their decomposition results in the production of char [10]. In addition to temperature, the thermal degradation of a material is highly dependent on the atmosphere in which it occurs. The presence of dioxygen greatly modifies the reaction kinetics, which generally accelerate although the opposite effect is sometimes observed [11]. but it can also induce the formation of new reaction products that would not be observed under an inert atmosphere [12]. Thermogravimetric analyses (TGA) conducted on PPS resin show that decomposition under inert atmosphere begins 20°C later than in air [11] but results in a slightly greater mass loss. When its formation is completed the char begins to decompose at a slow rate (12% in 300°C), as shown by Yao et al. who observed slow rate decomposition in PEEK-based composites [13]. Indeed pyrolysis (i.e. the first stage of decomposition) does lead to a greater mass loss under inert atmosphere, but this is only because it is completed. Conversely, due to oxidation, decomposition under air results in the total gasification of char at 750°C.

Second of all the presence of fibres in an organic matrix greatly influences thermal decomposition, since fibres have a higher thermal resistance than polymers. For example glass fibres begin to soften between 700 and 1000°C [14]. Carbon fibres have a particularly high thermal resistance with a sublimation temperature above 3000°C in an inert atmosphere. However they are very sensitive to oxidation with complete decomposition when the temperature rises to 950°C under air [15]. Under isothermal conditions the oxidation of carbon fibres starts at 500°C and results in their total decomposition in 3 hours at 650°C. A thermal degradation study was carried out by Tadini et al. [16] on carbon fibres reinforced composites (PEKK- and phenolic-based). To evaluate the PEKK behavior and to understand the impact of composite nature in terms of structural strength under fire TGA tests were performed under different non-isothermal heating conditions (between 30 and 1000°C). Under inert atmosphere PEKK-based composites are characterized by one single global reaction between 500–700°C. Phenolic-based composites are characterized by two reactions and earlier pyrolysis (around 200°C). The better performance of PEKK composites is attributed to the ether and ketone bonds between the three aromatic groups of the monomer.

1.2 Thermal decomposition of PPS

105 The anisothermal thermal decomposition of PPS has been specifically addressed by different authors [17-
106 25]. Depending on the heating rate, it starts between 450 and 500°C and initially leads to a mass loss of
107 between 45 and 65% depending on the considered atmosphere. The chemical mechanisms of this
108 decomposition were studied using different characterization techniques: Pyrolysis (Py) - Mass
109 Spectrometry (MS) [19], Gas Chromatography (GC) [20], Py-GC-MS and TGA-MS coupling [21], etc. Not
110 all studies agree on the chronology of chemical mechanisms probably because of the different formulations
111 of the PPS resin. Nevertheless the decomposition seems to be a competition between depolymerization and
112 random chain scission resulting in the formation of benzenethiol and hydrogen sulfide H_2S, carbon
113 disulfide CS_2 and benzene respectively [21,22]. Cyclisation reactions between different decomposition
114 products then lead to the formation of char [19]. The latter, like what is observed during the decomposition
115 of the PEEK, then undergoes a slow thermal decomposition, which results in a relatively small mass loss.
116 This observation is only true for decompositions in an inert atmosphere. Under air, char undergoes
117 oxidation leading to its complete volatilization before 800°C.
118
119 As shown by Patel et al. in PEEK-based composites, the first stage of pyrolysis is relatively unaffected by
120 the atmosphere [23]. When it comes to thermal decomposition, $T_{5\%}$ refers to the temperature at the onset of
121 decomposition often defined as the temperature corresponding to a mass loss of 5%. Nevertheless in PPS-
122 based composites, mechanisms of cross-linking under air, occurring at temperatures lower than $T_{5\%}$, can
123 increase the thermal resistance of PPS and delay the onset of its decomposition [24]. This phenomenon has
124 been highlighted by Ma et al. [11]. The study of isothermal decomposition between 410 and 470°C reveals
125 that from 440°C, the mass loss after 2 hours is higher under N_2 than under air (see Fig. 2b). This result
126 explains why mass loss begins later in TGA (anisothermal conditions) under air (see Fig. 2a). Note that the
127 inflection in the residual mass under air, which is a characteristic of a new decomposition mechanism (here
128 oxidation), is observed for residual mass of PPS around 75%, far before the end of pyrolysis under inert
129 atmosphere, suggesting an overlap of the two mechanisms.
130

1.3 Objectives of the study

The study of fire resistance aims to understand and characterize how and for how long the composite material can bear a mechanical loading when one face is subjected to heat fluxes. It results in temperature differences transversely on the sample exposed surface as well as through the materials thickness. The knowledge of the temperature distribution on both exposed and back surfaces is required to determine the temperature range within the materials with respect to its characteristic temperatures (glass transition, melting, pyrolysis onset). Before considering the combined influence of heat and mechanical loadings, it is also necessary to investigate the influence of temperature on the thermal decomposition of C/PPS composites and its constitutive materials depending on the testing conditions. Thus TGA tests were carried out for different heating rates, in both isothermal and anisothermal conditions, under inert or oxidizing atmospheres.

2. Material and methods

2.1 Materials and specimens

The studied composite materials are carbon fabric reinforced laminates consisting of a semi-crystalline high-performance PPS supplied by the Ticona company. The woven-ply prepreg, supplied by SOFICAR, consists of 5-harness satin weave carbon fiber fabrics (T300 3K 5HS) whose weight fraction is 58%. The prepreg plates are hot pressed according to a quasi-isotropic [(0,90)/(±45)/(0,90)/(±45)/(0,90)/(±45)/(0,90)] stacking sequence (see Fig. 3). The glass transition temperature of the material is T_g=98°C and its melting temperature T_m=280°C, as measured by DSC [26]. The degree of crystallinity of PPS matrix is close to 30% and the porosity ratio is very small (less than 2%).

2.2 Experimental set-up

2.2.1 Radiative heat flux exposure and temperature measurements

To study fire resistance a cone calorimeter is usually used. A rectangular sample (100*150mm² and a 2.2mm thickness) is placed under a fume hood and subjected to different heat fluxes (30-40-50kW/m²)

157 resulting from the radiation of a conical heating resistor. The temperature distribution within the material
158 must be measured in order to understand thermally-induced phenomena such as the thermal decomposition
159 and degradation of mechanical properties [27]. Temperature measurements are conducted on the exposed
160 and the back surfaces of the specimens. In the present study, two methods are used to measure the
161 temperature: by infrared thermography (back surface) or by means of thermocouples (exposed surface).
162 The first method is the most accurate because it provides the temperature mapping over the entire surface.
163 The infrared thermography measurement was carried out using a Thermacam camera PM 575
164 manufactured by FLIR Systems. To estimate the temperature, the camera requires the knowledge of the
165 material emissivity. The value was set at 0.90 according to the value frequently used in the literature for
166 composite materials with carbon fibres [28]. However infrared thermography measurement is difficult to
167 implement on the exposed surface because it requires the measurement of the temperature by observing the
168 specimen through the cone calorimeter. Such measurement presents many sources of errors: hot
169 atmosphere, pyrolysis gas, reflection of a part of the radiation on the surface of the sample. As a result type
170 K thermocouples are used to measure the temperature distribution on the exposed surface.
171

172 **2.2.2 Thermogravimetric Analysis (TGA)**

173 To carry out these experiments a thermo-gravimetric analyzer TA Instruments Discovery is used. Thermal
174 decomposition is characterized under three atmospheres: nitrogen, air and dioxygen. The gas flow rate is
175 set at 20 mL.min^{-1}.The extent of decomposition is characterized by a degree of progress in the reaction
176 defined by the following expression [29]:

177 $$\alpha = \frac{m_i - m}{m_i - m_f} \quad (1)$$

178 With m_i the initial mass of the sample, m is the mass at a time t and m_f is the mass after decomposition.
179 When the analysis is carried out in an inert atmosphere, α corresponds to the degree of pyrolysis and its
180 value is 1 when all the pyrolysis is completed. Under oxidizing atmosphere, it corresponds to the degree of
181 decomposition and its value is 1 when the entire solid residue is completely gasified.

The study of the PPS thermal decomposition has been conducted using anisothermal heating from room temperature to 700°C. These analyses are extremely useful for determining the primary steps of the decomposition: $T_{5\%}$ refers to pyrolysis onset, which is the temperature at which 5% of the polymer mass has decomposed and T_{max} refers to the maximum peak of decomposition rate. Such analyses can also be considered for studying the thermal decomposition kinetics. However they are not suitable for clearly identifying the chemical mechanisms involved. Two types of analyses were conducted on samples whose initial mass is about 8mg:

- Anisothermal conditions at a heating rate of 10°C/min: linear evolution of temperature as a function of time. These experiences are supposed to be representative of the increase in material temperature during the transient phase of its thermal response.
- Isothermal conditions at a heating rate of 100°C/min: rapid temperature increase to a value of which is maintained for a period of 1h30 and 5h, depending on the test temperature. These experiments aim to characterize decomposition when the temperature of the material has reached its permanent state.

2.2.3 Modulated TGA

Derived from the modulated DSC analyses proposed by Flynn [29] and Reading [30], the MT–TGA method consists in subjecting a sample to a sinusoidal temperature ramp. It depends on the evolution of the degree of conversion between the peak (maximum heating rate) and the trough (minimum velocity) of a cycle. The activation energy E_a can be calculated [31] and related to the main decomposition mechanisms from a single experiment [32,33]:

$$E_a = \frac{R\,(T^2 - A^2)\,\mathrm{Ln}\left(\frac{d\alpha_p}{d\alpha_v}\right)}{2\,A} \qquad (2)$$

Where T is the average value of oscillatory temperature; A is the amplitude of the temperature oscillation; and $\frac{d\alpha_p}{d\alpha_v}$ is the ratio for adjacent peaks and valleys, of the periodic rate of reaction. The modulation parameters were: amplitude = 5K, period = 200s and heating rate = 5K/min.

3. Results and discussion

3.1 Radiative heat flux exposure

On the exposed and the back surfaces the changes in the surface temperature depend on the applied heat flux. The thermal response starts with a transient phase during which the temperature increases rapidly. On both surfaces temperature eventually becomes constant when the balance is reached between heat sources (radiation from the heat source) and losses (radiation of the material, convection and thermal decomposition). The lower the heat flux is, the longer it takes to reach this steady state (see Fig. 5a). Finally, by comparing the temperature profiles on both exposed and back surfaces of C/PPS laminates subjected to 50kW/m² heat flux, the through-the-thickness temperature difference can be estimated (see Fig. 4). In the steady state a significant difference (about 320°C) is observed through-the-thickness but also on the back surface (see Fig. 5b). The onset of decomposition temperature is reached on the exposed surface but not on the back surface. It is therefore reasonable to assume that the temperature profile through-the-thickness is nonlinear and that the laminates thickness increases as the material decomposes. The knowledge of the temperature difference is of the utmost importance to determine: (i) the gradient in both thermal and mechanical properties, (ii) gradient in the chemical composition, (iii) thermally-induced damages.

To better understand the influence of a heat flux on the temperature difference on the outer surfaces and within the laminates it is necessary to investigate the influence of temperature on the thermal decomposition of C/PPS composites and its constitutive materials depending on the testing conditions (see Fig. 1). TGA provides information on the temperatures at which the matrix is pyrolyzed and possibly at which the char and then the fibres oxidize in the composite. This will be useful in the future to establish a temperature profile according to thickness. Thus, TGA experiments were carried out in both isothermal and anisothermal conditions, under inert or oxidizing atmospheres (see Fig. 1) to identify the characteristic temperatures on the outer surfaces as well as within the materials.

3.2 TGA under anisothermal conditions

3.2.1 Inert atmosphere

Under nitrogen the pyrolysis of the PPS starts at 503°C and ends around 640°C resulting in a mass loss of about 55% (Figure 6a). Over this temperature range the evolution of the decomposition rate or Mass Loss Rate (often abbreviated MLR) has a virtually symmetrical peak with a maximum close to 550°C (Figure 6b). The presence of a single peak may indicate that pyrolysis occurs according to a meta-mechanism, a combination of random chain scission and depolymerization failures (see Section 1.1). The product of this decomposition, representing 45% of the initial mass, is char which is resistant at high temperatures with a mass loss of only 11% at 900°C (5% of the initial polymer mass – see Fig. 6a).

In C/PPS, consisting of 43% by weight of PPS, pyrolysis only results in a mass loss of 26% with a maximum decomposition rate at 550°C. Indeed the thermal decomposition of carbon fibres under inert atmosphere does not occur at this temperature level [15]. It is thus possible to calculate the mass loss of the matrix in the composite material, as well as its decomposition rate, assuming that only it decomposed while the fibres remained intact. It is interesting to note that despite the high thermal resistance of carbon fibers the decomposition of the matrix starts 20°C earlier in the composite material ($T_{5\%}$= 483°C at 10°C/min) as fibre/matrix interfaces are preferential areas for initiating a degradation mechanism. It could also be caused by the higher thermal conductivity of carbon fibres compared to the PPS matrix, bringing heat in the sample at a faster rate. Decomposition is also slightly more extensive with a polymer residual mass after pyrolysis of 60% compared to only 55% in the plain PPS. The presence of fibres also results in a decomposition rate of the matrix slower than for the resin alone (Figure 7a). The residue, consisting of char and fibres, is also very different from the decomposition of the plain PPS. Fibres limiting the swelling associated with the formation of pyrolysis gas, the residue of C/PPS is a highly porous fibrous network but only slightly thicker than the composite at room temperature (see Fig. 8a) while the product of the decomposition of the PPS (see Fig. 8b) is in the form of a bubble resulting from the "swelling" of the

material under high internal pressure. Although fibres do not decompose they have a significant influence on matrix decomposition.

Another illustration of this phenomenon concerns the evolution of the activation energy of decomposition mechanisms as a function of the pyrolysis degree [32, 33], studied here by modulated TGA (Figure 7b). Comparison of curves $\boldsymbol{E_a = f(\alpha)}$ shows that the activation energy required to initiate decomposition (α < 0.1) is much lower in the case of C/PPS, which could explain why it takes place at a lower temperature. During most of the decomposition, $\boldsymbol{E_a}$ is higher for PPS alone resulting in an ever higher decomposition rate (Figure 7a). Finally, we can observe that the last peak of activation energy, associated with char formation, starts later in C/PPS ($\boldsymbol{\alpha}$ =0.84 compared to 0.76 for matrix). This may explain the lower residual polymer mass in the case of PPS only. The curves representing the activation energy is divided into three parts supposedly associated with the mechanisms of PPS pyrolysis: depolymerization, random chain scission and ultimately cyclisation through char formation.

3.2.2 Oxidizing atmosphere (Dioxygen and air)

As indicated in section 1.1 the decomposition of carbon fibre-reinforced composites under oxidizing atmosphere is faster than the one of other fibers-reinforced composites such as glass fibres for example, because carbon fibres are sensitive to oxidation phenomena just like polymeric matrices. For practical reasons decomposition under air has been little studied. The oxidation phenomena are here mainly characterized with TGA analyses under dioxygen.

Under dioxygen, the thermal decomposition of PPS begins at 502°C, approximately the same temperature as under an inert atmosphere (see Table 1). The curve representing the Mass Loss Rate of plain PPS resin as a function of temperature *MLR = f(T)* is characterized by 3 peaks (see Figure 9). The first peak corresponds to a mass loss of about 15%. Thus it may be associated with the first pyrolysis mechanism, depolymerization (Figure 10b). Following this reasoning, the second peak, which extends to $\boldsymbol{\Delta m = 37\%}$, may be associated with the second pyrolysis mechanism. Even before the pyrolysis ends a new mechanism starts and may be associated with the simultaneous oxidation of PPS matrix and the pyrolysis residue as it

extends until the entire initial material is carbonated (Figure 10a). The maximum oxidation rate is virtually 3 times higher than the pyrolysis rate.

In C/PPS thermal decomposition begins at 515°C, i.e. 10°C later than under N_2 (see Table 1). Similar observations have already been made by Ma et al. in the study of the decomposition of C/PPS under air and can be explained by the behaviour thermoplastic-thermosetting PPS [11]. Indeed when heated in an oxidizing atmosphere above its melting temperature PPS can crosslink like a thermosetting polymer thus having a higher thermal stability. If the delay in the onset of decomposition is only observed in C/PPS composite, this suggests that these phenomena are promoted by the presence of fibres. As for the PPS matrix alone pyrolysis and oxidation of char overlap in the C/PPS. Nevertheless the fact that the second peak of MLR ends with a mass loss of 43% equivalent to the matrix mass in the composite, it tends to indicate that oxidation of char and fibres occurs separately and not simultaneously (Figure 10a). Analysis of the evolution of the activation energy E_a indicates a rather good correlation with decomposition rate except when the material is strongly degraded as the MLR decreases with E_a. It is also possible to infer that the oxidation mechanisms are broken down into several sub-mechanisms represented by different peaks on the Ea vs polymer mass loss (Figure 10b). Finally, pyrolysis under oxidizing atmospheres requires higher Ea than under nitrogen, which might be consistent with the cross-linking hypothesis (Figure 11).

The decomposition of PPS begins at 508°C at 20°C/min under air, which is the only experimental condition tested under this atmosphere. For the same heating rate, decomposition begins at 523°C and 530°C respectively under N_2 and O_2 (see Table 2). Pyrolysis results in a mass loss of 39%, which is lower than that observed under inert atmosphere (Figure 12a), which is consistent with the observations made in the case of a PEEK resin by Patel et al [23][34]. As under dioxygen, oxidation begins before the pyrolysis ends. Nevertheless the appearance of the characteristic peak of pyrolysis on the MLR curve $MLR = f(T)$ indicates that pyrolysis is almost completed when oxidation begins under air (Figure 12b) while it did not even reach its maximum rate when this transition occurs under O_2. In C/PPS, decomposition begins at 517°C compared to 525 and 526°C under N_2 and O_2 (see Table 2).Thus the mechanisms of crosslinking and improvement of thermal resistance observed under O_2 do not appear to occur under air. During isothermal

tests under air, the latter have not been observed in C/PPS by Ma et al. However the decomposition temperatures cannot be readily discussed from one atmosphere to another as the operating conditions differ in term of heating rate and testing machine. Oxidation appears to start faster under O_2 simply because there are more reactive species and the atmosphere is more oxidizing.

3.3 TGA under isothermal conditions

3.3.1 Inert atmosphere

The isothermal decomposition of C/PPS under N_2 was studied for a temperature range between 465 and 545°C. Lower temperatures than in an oxidizing atmosphere were chosen. Indeed the inert atmosphere is representative of what the specimen undergoes at core whose temperature is lower than that of the exposed side subjected to an oxidizing atmosphere (see Fig. 1b). In addition the temperature profiles measured in section 3.1 are considered here to justify the choice of isothermal temperature conditions. As expected the mass losses are at least equal to or greater than those observed during anisothermal decomposition (Figure 13) for all test temperatures except one (530°C). At 465°C for example, while only 2% of the mass of polymer in C/PPS are gasified under anisothermal conditions, mass loss reaches 12% (28% of the matrix) after 30 minutes of exposure and 29% (69% of the matrix) at the end of the test. The higher the test temperature, the higher the mass loss. Indeed whereas for high temperatures (530 and 545°C), the mass loss seems to reach a plateau, which is not the case for lower temperatures (at least over the temperature range studied). However the isothermal conditions are not really isothermal for the highest temperatures at which the decomposition has already clearly started at lower $T_{5\%}$ decomposition temperatures (whose accurate estimate is difficult), which calls into question the possibility of direct comparison.

3.3.2 Oxidizing atmosphere (Dioxygen and air)

Under oxidizing atmosphere isothermal decomposition was studied for four temperatures: 520, 550, 580 and 610°C. The second and fourth were chosen because these are the maximum temperatures measured on

the front panel for specimens of C/PPS exposed to flux densities of 40 and 50 kW/m2 (see Section 3.1). One of the difficulties of the analysis is that the material can be quite significantly decomposed during the temperature rise up to the test temperature. Nevertheless this temperature ramp is partially representative of what the material undergoes during fire exposure and thus contributes to the understanding of fire behaviour. Fire exposure combines both radiative and convective fluxes leading to heat fluxes higher than 100kW/m², whereas the fluxes resulting from cone calorimeters are usually lower than 80kW/m². The oxidizing atmosphere in the vicinity of the surface exposed to a cone calorimeter allows the combustion of pyrolysis gases. On the contrary, there is very little dioxygen in the vicinity of the sample surface exposed to a flame. Under real fire conditions, it is therefore expected that the thermal decomposition of C/PPS laminates would differ from the one observed under a radiative heat flux.

As under inert atmosphere, the same decomposition mechanisms as under anisothermal conditions may be at stake. However the times required for decomposition are shorter than under N_2 (Figure 14). The distribution of decomposition rate peaks and therefore the decomposition mechanisms change with temperature. For example, under the air, the lower the temperature, the more pyrolysis is characterized by a low mass loss (Figure 15). The air crosslinking mechanisms highlighted by Ma et al. could partly explain this phenomenon [11]. However this is no longer true when pyrolysis starts. For lower temperatures, as the PPS matrix decomposition is slow, a partial crosslinking of the matrix occurring at the same time could result in less extensive pyrolysis and therefore explain an earlier oxidation. Decomposition rates differ under the two atmospheres. Under air, they are approximately 4 times lower than those observed under O_2, which can be related to the percentage of dioxygen in the air. The fastest mechanisms are also different under both atmospheres. Under air, pyrolysis occurs more rapidly while under dioxygen it is the oxidation of char that occurs faster.

4. Conclusion

The investigations on the relationship between local temperature resulting from the local balance energy exchange, the local atmosphere and the mass losses are essential in understanding the influence of fire on polymers and polymer matrix composites. The main objective of this work was to better understand the thermal decomposition mechanisms in both PPS plain resin and PPS thermoplastic-based composites subjected to radiative heat fluxes representative of fire exposure.

The first step consisted in investigating the influence of thermal heat fluxes (hence temperature) resulting from fire of medium intensity. Such heat fluxes (typically 50kW/m²) lead to significant thermal gradients within composite structures, leading to (i) a gradient in both thermal and mechanical properties, (ii) a gradient of chemical composition and (iii) thermally induced damages.

By comparing the temperature profiles on both exposed and back surfaces of C/PPS laminates subjected to a 50kW/m² heat flux, the through-the-thickness temperature gradient has been shown to be significant (about 320°C in the steady state). For such temperature level, the onset of decomposition temperature is reached on the exposed surface but not on the back surface, leading to a significant gradient of the chemical composition through the thickness.

In order to predict the evolution of properties for other heat fluxes, decomposition mechanisms as well as their kinetics and their activation energy under different heating conditions (isothermal and anisothermal), or testing atmosphere (inert and oxidizing), have been studied by means of TGA and MT-TGA tests. If the influence of the atmosphere has shown similar behaviors to what is conventionally observed on other materials and corroborated by other studies on the PPS [21][31], questions were raised about the influence of the heating rate in anisothermal conditions. Even if the heating rates tested in this study (10 and 20°C/min) are low compared to those observed in a real fire (several hundred degrees per minute),

386 differences were observed in the increase of $T_{d,onset}$ when the heating rate increases, whether the testing
387 atmosphere is oxidizing or not.
388
389 Considering the influence of heating conditions in isothermal conditions, an increase in the testing
390 temperature leads to increasing decomposition rates, as expected. Oxidation starts before the end of
391 pyrolysis under anisothermal conditions, whereas pyrolysis is complete before oxidation under isothermal
392 conditions. As far the influence of fibers on the thermal decomposition mechanisms in PPS-based
393 composites is concerned, the cross-linking may be promoted by the presence of fibers resulting in delaying
394 the onset of pyrolysis under oxidizing atmosphere. Such cross-linking is not significant enough to observe
395 such a delay under air. In agreement with conclusions drawn in the literature on PPS and PPS-based
396 composites, MT-TGA tests suggest the existence of three different mechanisms during pyrolysis under
397 inert atmosphere: depolymerization, random chain scission and ultimately cyclisation (char formation).
398

399 **References**

400 [1] A.P. Mouritz, A.G. Gibson. Fire properties of polymer composite materials. N° 143 Solid mechanics
401 and its applications. Springer, Dordrecht, 2006.
402 [2] T.N.A. Browne. A model for the structural integrity of composite laminates in fire. PhD doctoral
403 dissertation, University of Newcastle upon Tyne, 2006.
404 [3] A.G. Gibson, M.E.O. Torres, T.N.A. Browne, S. Feih, A.P. Mouritz. High temperature and fire
405 behaviour of continuous glass fibre/polypropylene laminates.
406 Composites Part A : Applied Science and Manufacturing, 41(9):1219–1231, 2010.
407 [4] B. Vieille, A. Coppalle, C. Keller, M.-R. Garda, Q. Viel, E. Dargent. Correlation between post fire
408 behavior and microstructure degradation of aeronautical polymer composites. Materials and Design 2015;
409 74:76–85.
410 [5] Y. Bai, T. Keller. High temperature performance of polymer composites. Wiley- VCH, Weinheim,
411 2014. OCLC: 864518902.

412 [6] B. Vieille, C. Lefebvre, A. Coppalle. Post fire behavior of carbon fibers Polyphenylene Sulfide- and
413 epoxy-based laminates for aeronautical applications: A comparative study. Materials and Design 2014;
414 63:56–68.
415 [7] E. Guillaume. Modélisation de la décomposition thermique des matériaux en cas d'incendie.
416 Techniques de l'ingénieur, 2013.
417 [8] D. Drysdale. An introduction to fire dynamics. John Wiley & Sons, 2011.
418 [9] N. Grange, P. Tadini, K. Chetehouna, N. Gascoin, I. Reynaud, S. Senave. Determination of
419 thermophysical properties for carbon-reinforced polymer-based composites up to 1000°C. Thermochimica
420 Acta 2016; doi: 10.1016/j.tca.2017.11.014.
421 [10] A. F. Grand, C. A. Wilkie. Fire retardancy of polymeric materials. Marcel Dekker, New York, 2000.
422 [11] C.-C.M. Ma, H.-C. Hsia, W.-L. Liu, J.-T. Hu. Studies on Thermogravimetric Properties of
423 Polyphenylene Sulfide and Polyetherether Ketone Resins and Composites. Journal of Thermoplastic
424 Composite Materials 1988; 1(1):39–49.
425 [12] D. Price, A.R. Horrocks. Polymer degradation and the matching of FR chemistry to degradation. In
426 Fire retardancy of polymeric materials, pages 15–42. Marcel Dekker, New York, 2000.
427 [13] F. Yao, J. Zheng, M. Qi, W. Wang, Z. Qi. The thermal decomposition kinetics of poly(ether-ether-
428 ketone) (PEEK) and its carbon fiber composite. Thermochimica Acta 1991. 183:91–97.
429 [14] A. Berthereau, E. Dallies. Fibres de verre de renforcement. Techniques de l'ingénieur, 2008.
430 [15] S. Feih, A. P. Mouritz. Tensile properties of carbon fibres and carbon fibre–polymer composites in
431 fire. Composites Part A : Applied Science and Manufacturing 2012, 43(5):765–772.
432 [16] P. Tadini, N. Grange, K. Chetehouna, N. Gascoin, S. Senave, I. Reynaud. Thermal degradation
433 analysis of innovative PEKK-based carbon composites for high-temperature aeronautical components.
434 Aerosp Sci Technol 2017; 65:106–16. doi:10.1016/j.ast.2017.02.011.
435 [17] G.F. Ehlers, K.R. Fisch, W.R. Powell. Thermal degradation of polymers with phenylene units in the
436 chain. I. Polyphenylenes and poly(phenylene oxides). J. Polym. Sci. A-1 Polym. Chem. 1969; 7: 2931-
437 2953.

438 [18] N.S. Christopher, J.L. Cotter, G.J. Knight, W.W. Wright. Thermal degradation of poly(phenylene
439 sulfide) and perfluoropoly(phenylene sulfide). J. Appl. Polym. Sci. 1968; 12: 863-870.
440 [19] G. Montaudo, C. Puglisi, F. Samperi. Primary thermal degradation processes occurring in
441 poly(phenylenesulfide) investigated by direct pyrolysis–mass spectrometry. Journal of Polymer Science
442 Part A: Polymer Chemistry 1994, 32(10):1807–1815.
443 [20] D.R. Budgell, M. Day, J.D. Cooney. Thermal degradation of poly(phenylene sulfide) as monitored by
444 pyrolysis—GC/MS. Polym Degrad Stab 1994;43:109–15.
445 [21] L.H. Perng. Thermal decomposition characteristics of poly(phenylene sulfide) by stepwise Py-GC/MS
446 and TG/MS techniques. Polym Degrad Stab 2000; 69: 323–32.
447 [22] O.A. Peters, R.H. Still. The thermal degradation of poly(phenylene sulphide) - Part 1. Polymer
448 Degradation and Stability 1993; 42(1):41–48.
449 [23] P. Patel, T.R. Hull, R.W. McCabe, D. Flath, J. Grasmeder, M. Percy. Mechanism of thermal
450 decomposition of poly(ether ether ketone) (PEEK) from a review of decomposition studies. Polymer
451 Degradation and Stability 2010; 95(5):709–718.
452 [24] R. T. Hawkins. Chemistry of the Cure of Poly(p-phenylene sulfide). Macromolecules 1976; 9(2):189–
453 194.
454 [25] X.-G. Li, M.-R. Huang, H. Bai, Y.-L. Yang. High-resolution thermogravimetry of polyphenylene
455 sulfide film under four atmospheres. Journal of Applied Polymer Science, 2002; 83(10):2053–2059.
456 [26] D. Blond, B. Vieille, M. Gomina, L. Taleb. Correlation between physical properties, microstructure
457 and thermo-mechanical behavior of PPS-based composites processed by stamping. Journal of Reinforced
458 Plastics and Composites 2014; 33(17): 1656-1668.
459 [27] Y. Carpier, B. Vieille, M.A. Maaroufi, A. Coppalle, F. Barbe. Mechanical behavior of carbon fibers
460 polyphenylene sulfide composites exposed to radiant heat flux and constant compressive force. Composite
461 Structures 2018; 200: 1-11.
462 [28] P. Boulet, D. Brissinger, A. Collin, Z. Acem, G. Parent. On the influence of the sample absorptivity
463 when studying the thermal degradation of materials. Materials 2015; 8(8):5398–5413.

464 [29] J.H. Flynn. The historical development of applied nonisothermal kinetics. In Thermal Analysis,
465 Volume 2, pages 1111–1126. R.F. Schwenker and P.D. Garn, New York, 1969.
466 [30] M. Reading, D.J. Hourston. Modulated Temperature Differential Scanning Calorimetry: Theoretical
467 and Practical Applications in Polymer Characterization. Springer Science & Business Media, 2006.
468 [31] R.L. Blaine, B.K. Hahn. Obtaining Kinetic Parameters by Modulated Thermogravimetry. Journal of
469 Thermal Analysis and Calorimetry 1998; 54(2):695–704.
470 [32] K. Cheng, W.T. Winter, A.J. Stipanovic. A modulated-TGA approach to the kinetics of lignocellulosic
471 biomass pyrolysis/combustion. Polymer Degradation and Stability 2012; 975(9): 1606-1615.
472 [33] C.A. Gracia-Fernández, S.Gómez-Barreiro, S. Ruíz-Salvador, R. Blaine. Study of the degradation of a
473 thermoset system using TGA and modulated TGA. Progress in Organic Coatings 2005; 54(4):332-336.
474 [34] P. Patel, T.R. Hull, R. E. Lyon, S.I. Stoliarov, R.N. Walters, S. Crowley, N. Safronava. Investigation
475 of the thermal decomposition and flammability of PEEK and its carbon and glass-fibre composites.
476 Polymer Degradation and Stability 2011; 96(1):12–22.
477
478
479
480

List of figure

Fig. 1 – Physico-chemical processes and phase distribution during the thermal decomposition of: (a) thermoplastic matrix (adapted from [7]) – (b) TP-based composites

Fig. 2 – (a) Anisothermal thermal decomposition of PPS and C/PPS (b) Isothermal thermal decomposition of PPS (according to [11])

Fig. 3 – Through-the-thickness microscopic observation of the mesotructure in quasi-isotropic C/PPS laminates

Fig. 4 – Temperature changes in C/PPS samples subjected to a radiant heat flux (50kW/m²)

Fig. 5 – Temperature measurements on the back surface by means of infrared thermography:
(a) Influence of heat flux (at specimen center) - (b) Temperature distribution at 50kW/m² (after t=180s)

Fig. 6 – (a) TGA curves of PPS and C/PPS under N_2 (b) Evolution of the decomposition rate as a function of temperature

Fig. 7 – Comparison of the decomposition of pure PPS or PPS associated with carbon fibres: (a) Decomposition rate as a function of pyrolysis degree α – (b) Activation energy of the pyrolysis reaction as a function of the degree of pyrolysis

Fig. 8 – Microscopic observations of TGA specimens after thermal decomposition under N_2:
(a) C/PPS – (b) PPS

Fig. 9 – Evolution of residual mass and decomposition rate (MLR) of PPS and C/PPS under O_2 as a function of temperature

Fig. 10 – (a) Evolution of the decomposition rate under O_2 as a function of the mass loss (b) Evolution of activation energy under O_2 as a function of polymer mass loss

Fig. 11 – Evolution of C/PPS activation energy under O_2 and N_2 as a function of mass loss

Fig. 12 – Decomposition of plain PPS and C/PPS composites at a heating rate 20°C/min:
(a) Residual mass and decomposition rate (MLR) under air in as a function of temperature (b) Decomposition rate as a function of degree of decomposition

506 Fig. 13 – Isothermal decomposition of C/PPS under inert atmosphere: (a) Evolution of the residual mass
507 over time (b) Decomposition rate in depending on the degree of pyrolysis
508 Fig. 14 – Isothermal decomposition of C/PPS as a function of time: (a) Under O_2 (b) Under air
509 Fig. 15 – Evolution of the decomposition rate as a function of the degree of pyrolysis:
510 (a) Under O_2 - (b) Under air

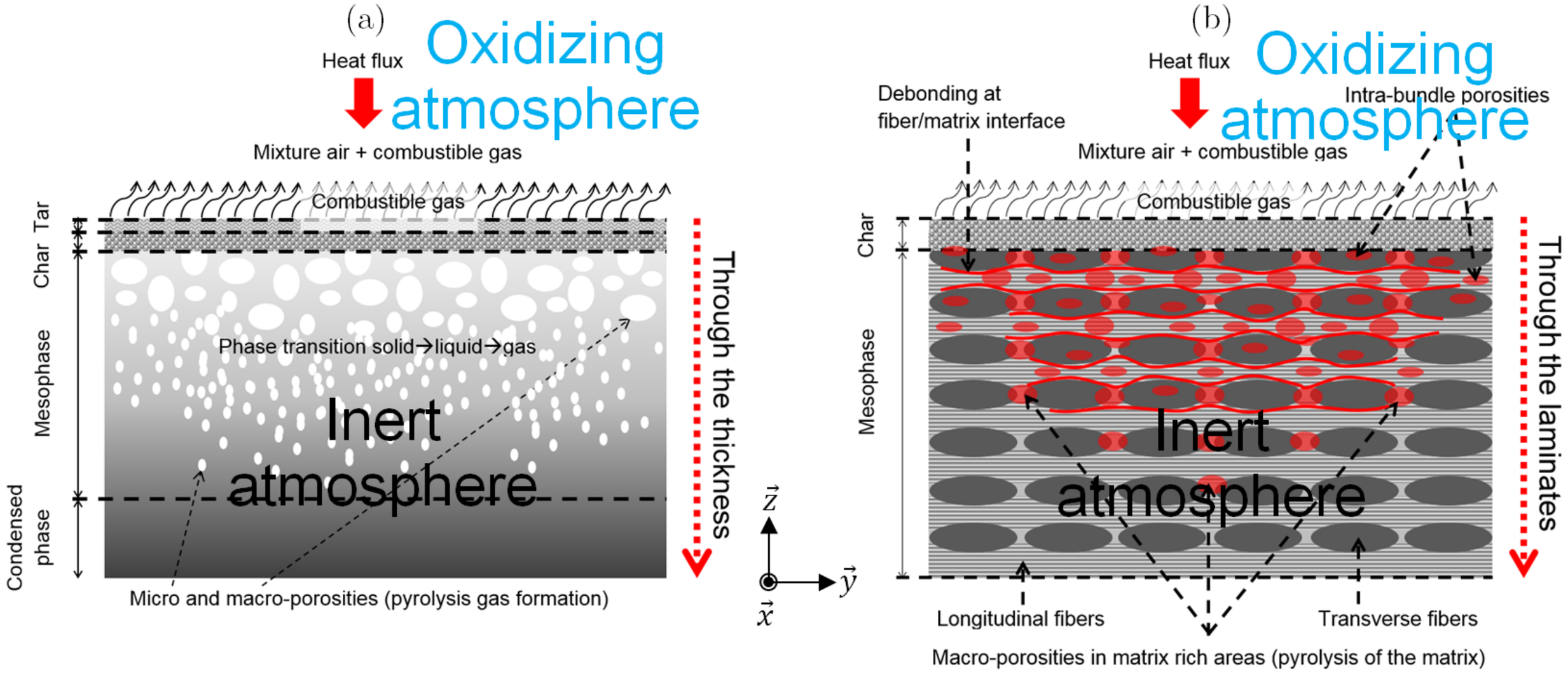
(a)
Heat flux
Oxidizing atmosphere
Mixture air + combustible gas
Combustible gas
Char
Tar
Mesophase
Condensed phase
Phase transition solid→liquid→gas
Inert atmosphere
Through the thickness
Micro and macro-porosities (pyrolysis gas formation)
(b)
Heat flux
Oxidizing atmosphere
Debonding at fiber/matrix interface
Intra-bundle porosities
Mixture air + combustible gas
Combustible gas
Char
Mesophase
Inert atmosphere
Through the laminates
Longitudinal fibers
Transverse fibers
Macro-porosities in matrix rich areas (pyrolysis of the matrix)

(a)

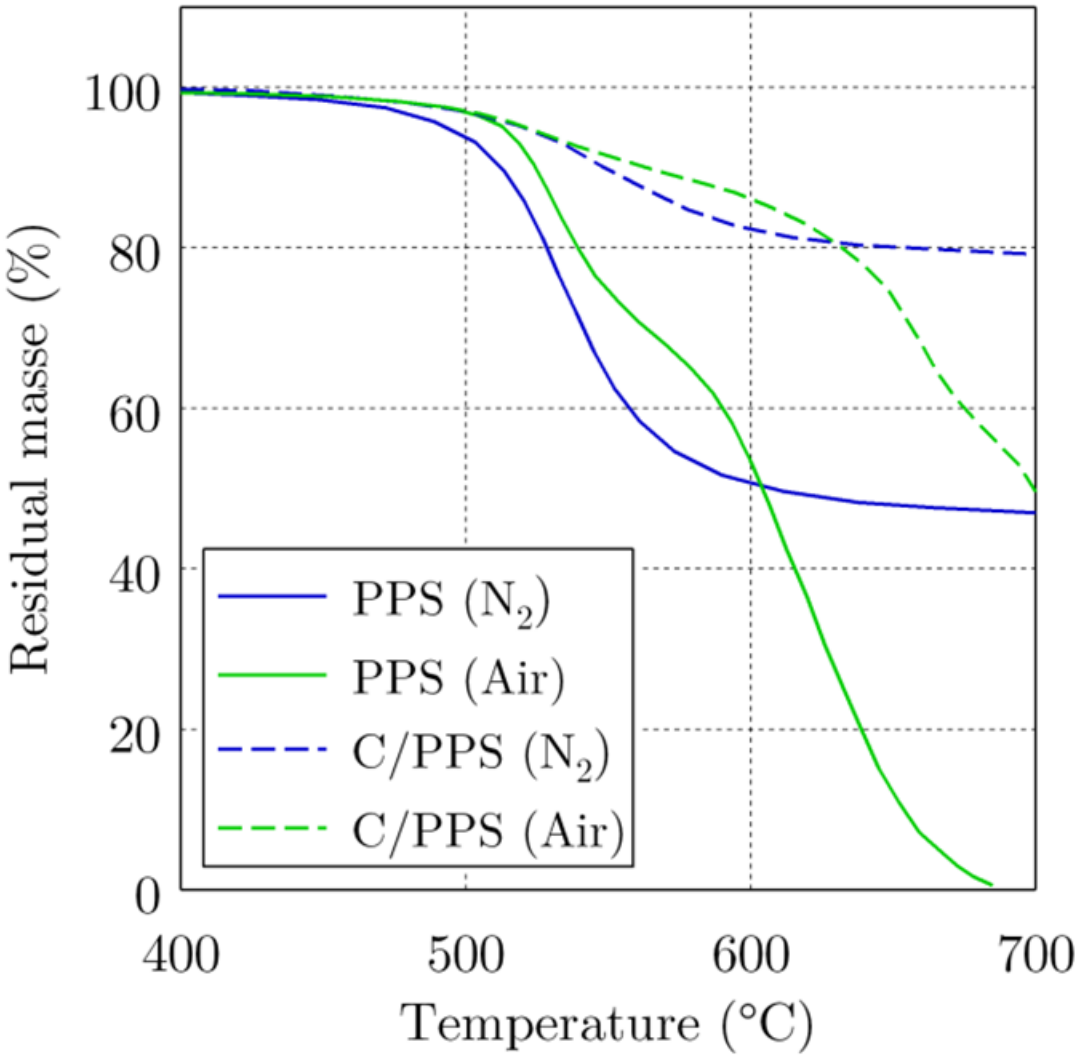
Residual masse (%)
100
80
60
40
20
0
400
500
600
700
Temperature (°C)
PPS (N2)
PPS (Air)
C/PPS (N2)
C/PPS (Air)

(b)

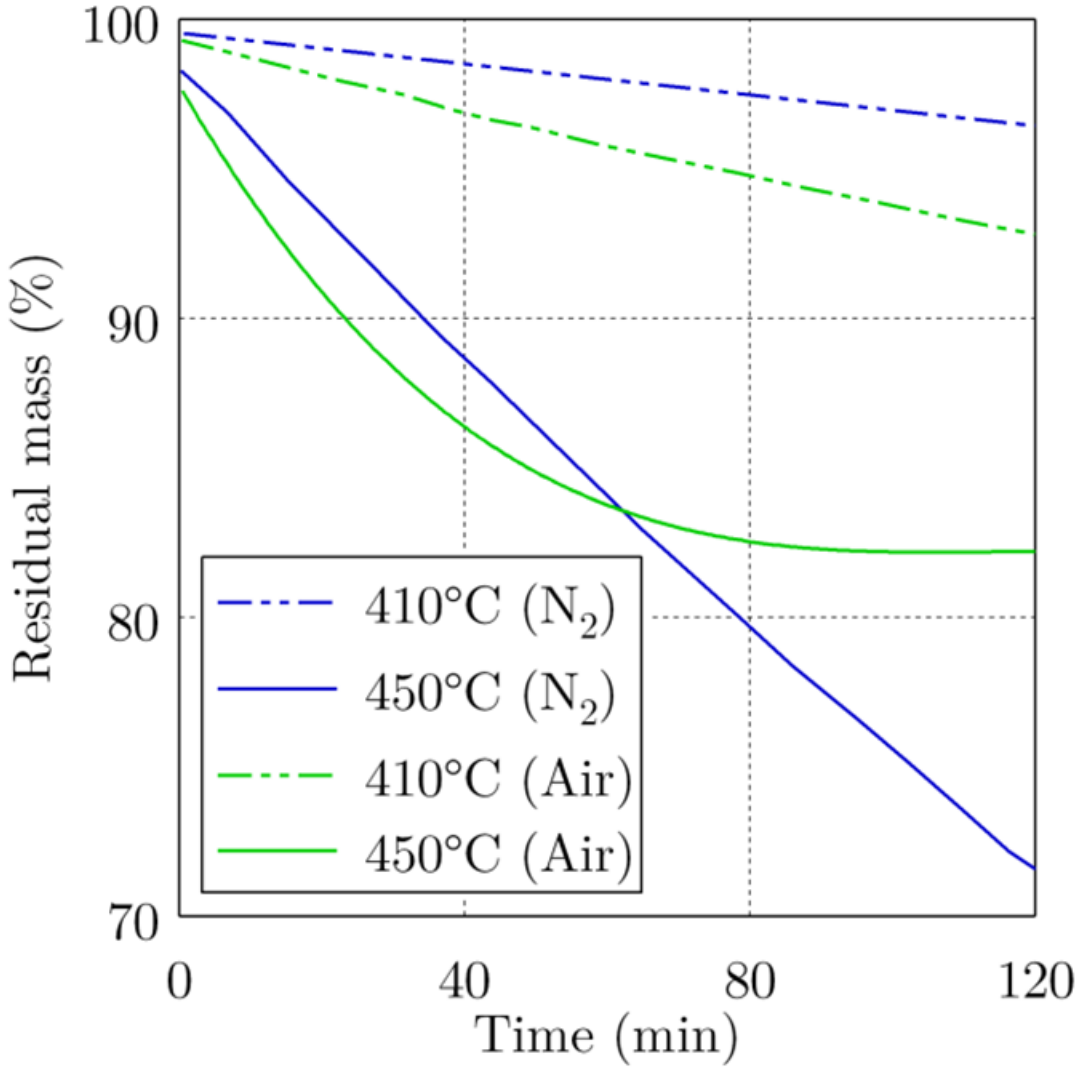
Residual mass (%)
100
90
80
70
0
40
80
120
Time (min)
410°C (N2)
450°C (N2)
410°C (Air)
450°C (Air)

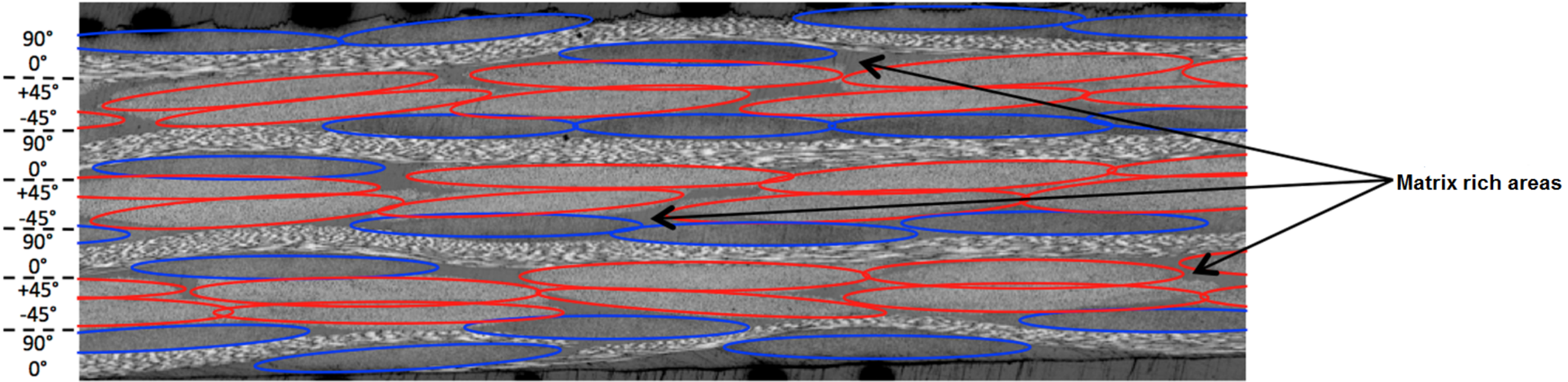
90°
0°
+45°
-45°
90°
0°
+45°
-45°
90°
0°
+45°
-45°
90°
0°
Matrix rich areas

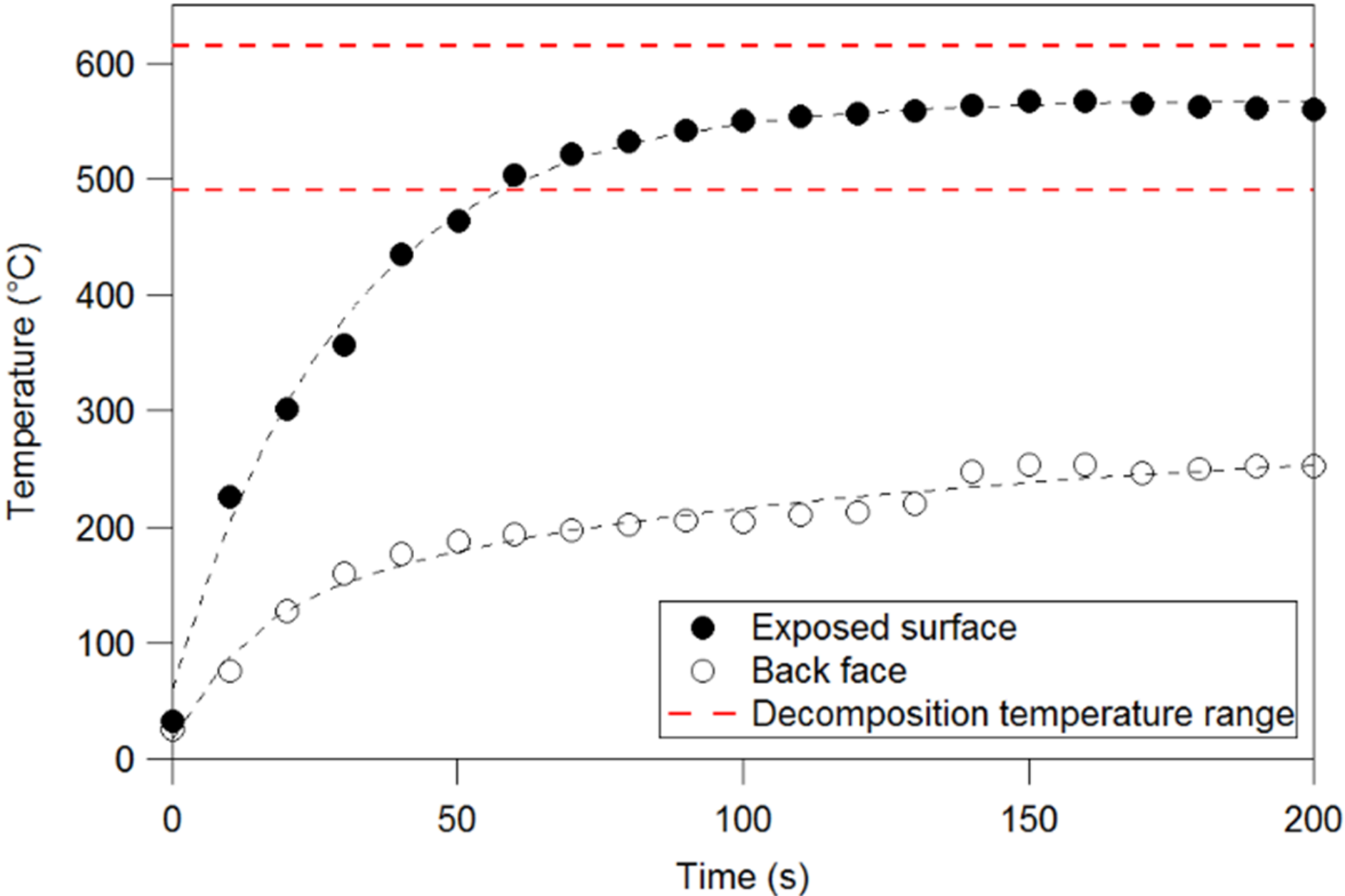
Temperature (°C)
600
500
400
300
200
100
0
0
50
100
150
200
Time (s)
Exposed surface
Back face
Decomposition temperature range

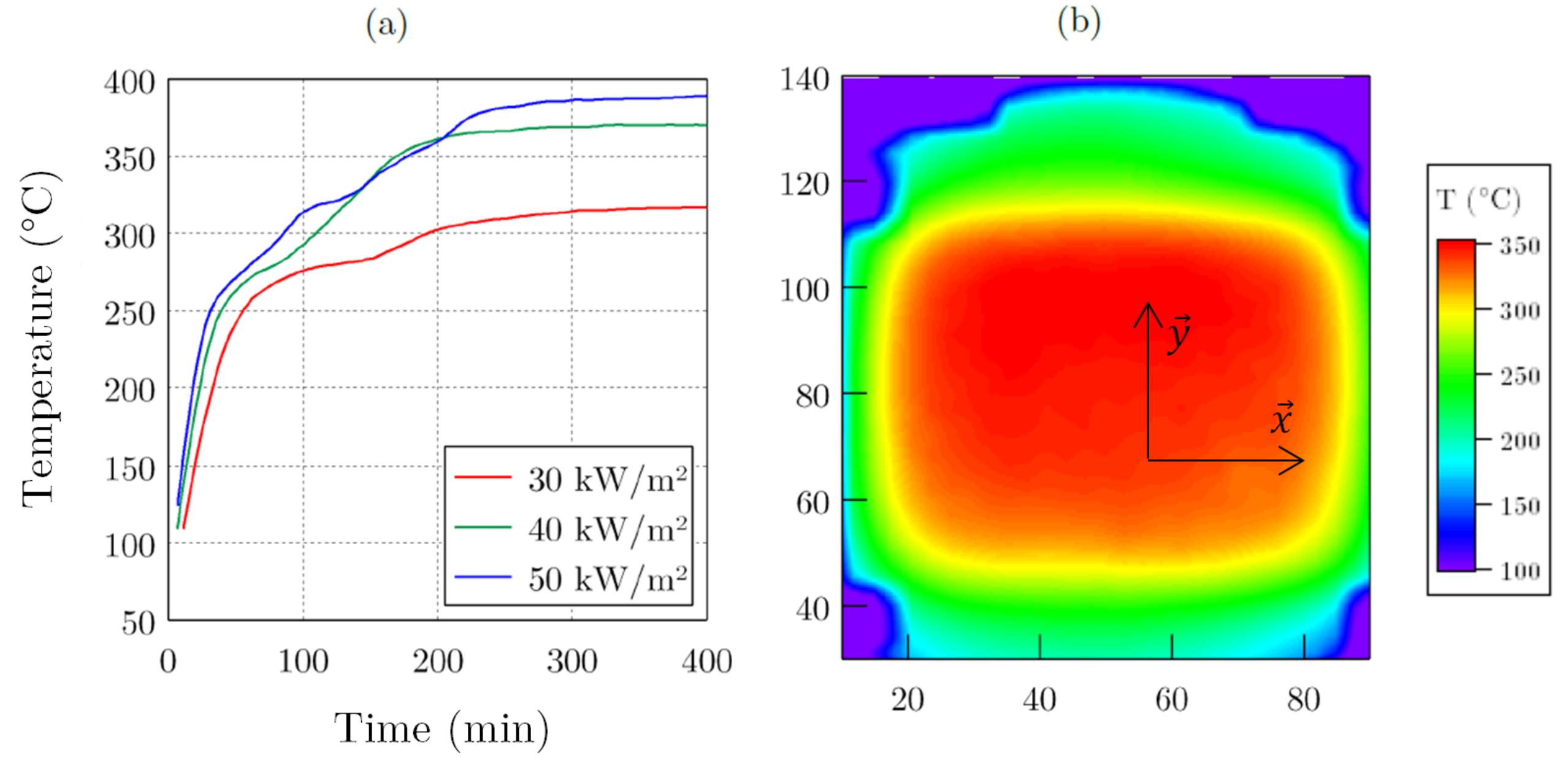
(a)
Temperature (°C)
400
350
300
250
200
150
100
50
0
100
200
300
400
Time (min)
30 kW/m²
40 kW/m²
50 kW/m²
(b)
140
120
100
80
60
40
20
40
60
80
$\vec{y}$
$\vec{x}$
T (°C)
350
300
250
200
150
100

(a)

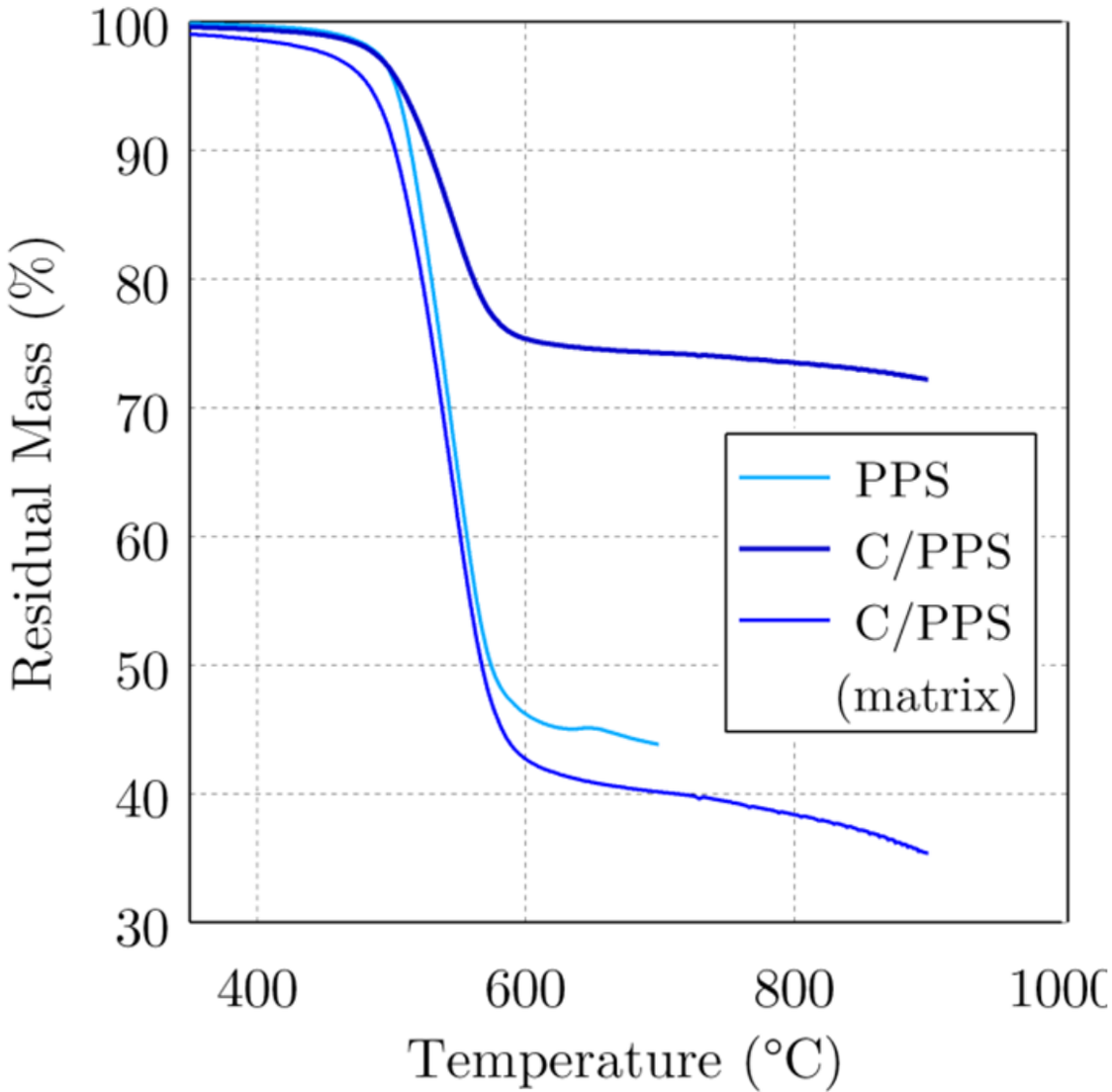
Residual Mass (%)
100
90
80
70
60
50
40
30
400
600
800
1000
Temperature (°C)
PPS
C/PPS
C/PPS
(matrix)

(b)

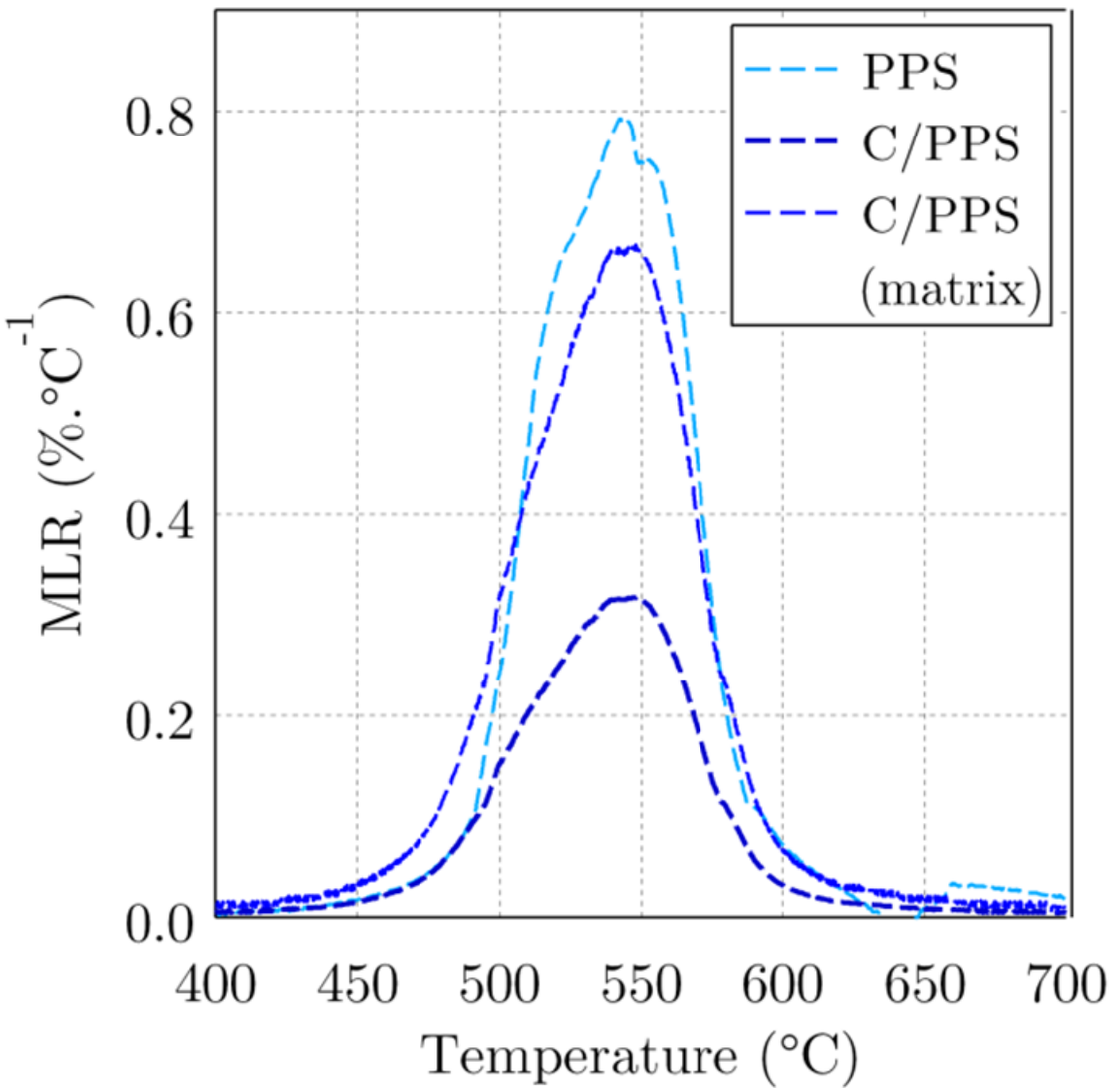
MLR (%.°C-1)
0.8
0.6
0.4
0.2
0.0
400
450
500
550
600
650
700
Temperature (°C)
PPS
C/PPS
C/PPS
(matrix)

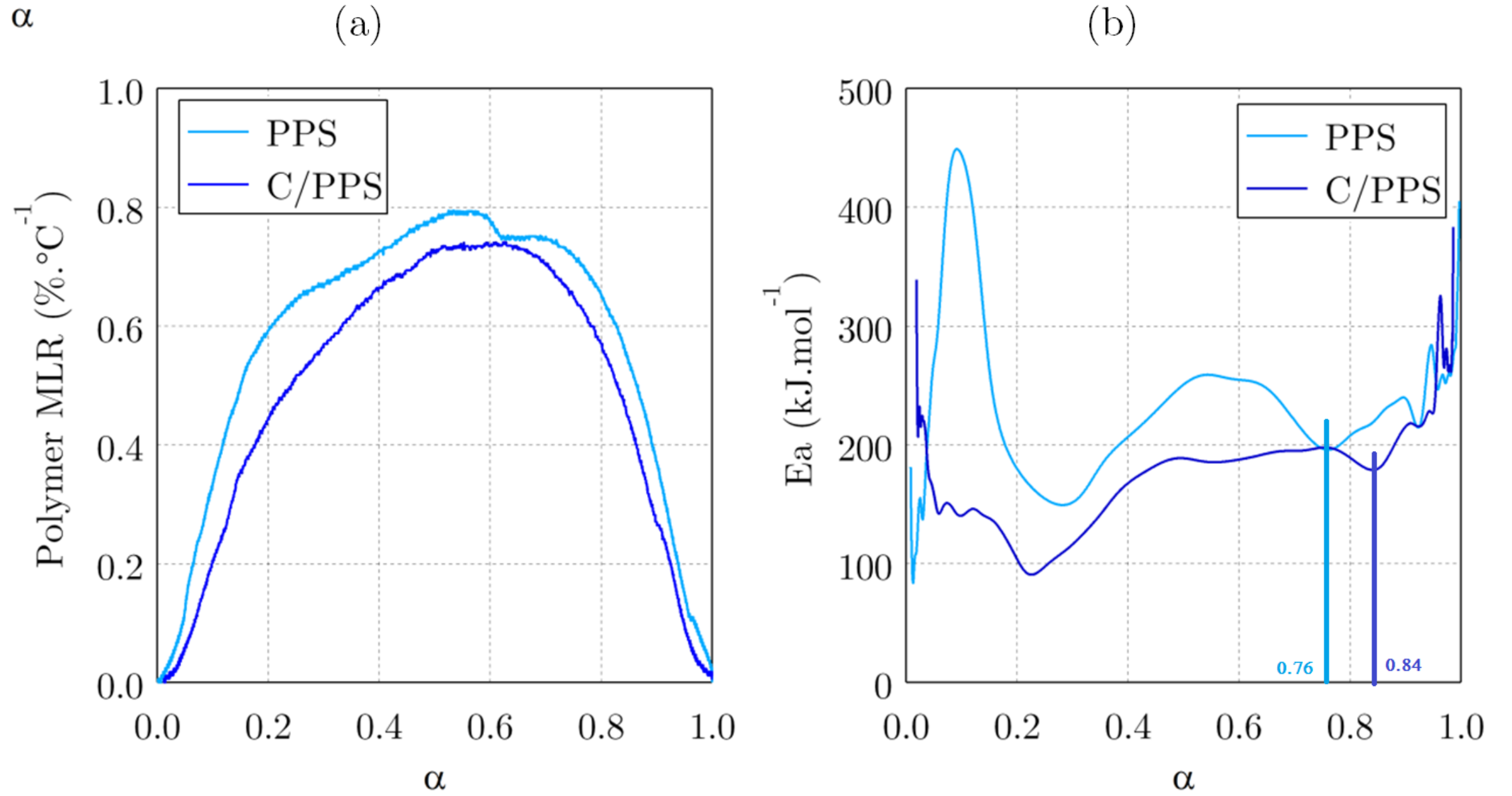
α
(a)
(b)
PPS
C/PPS
Polymer MLR (%.°C-1)
Ea (kJ.mol-1)
0.0
0.2
0.4
0.6
0.8
1.0
0
100
200
300
400
500
0.76
0.84
α
α

(a)

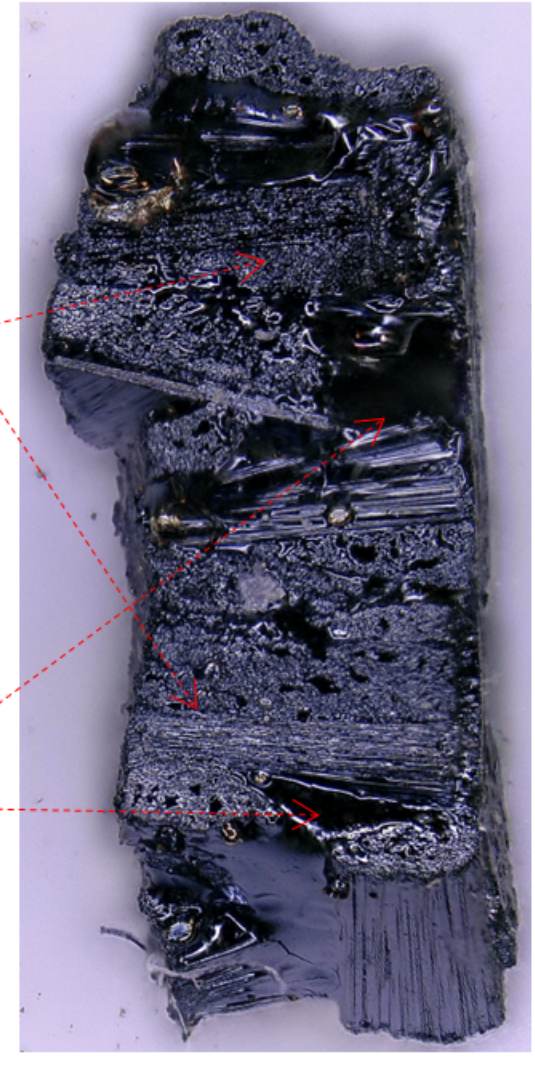
Carbon fibres
Melt PPS matrix
500µm

(b)

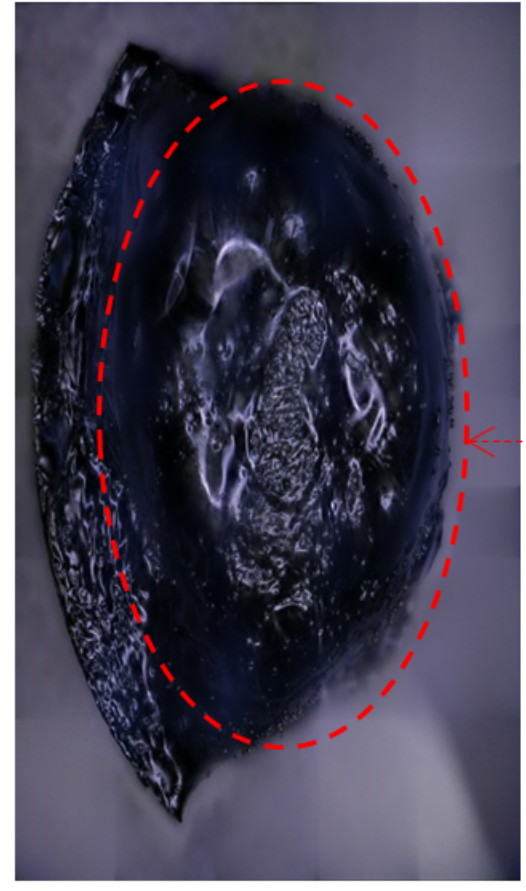
Bubble of melt PPS resin (swelling of pyrolysis gas)
1mm

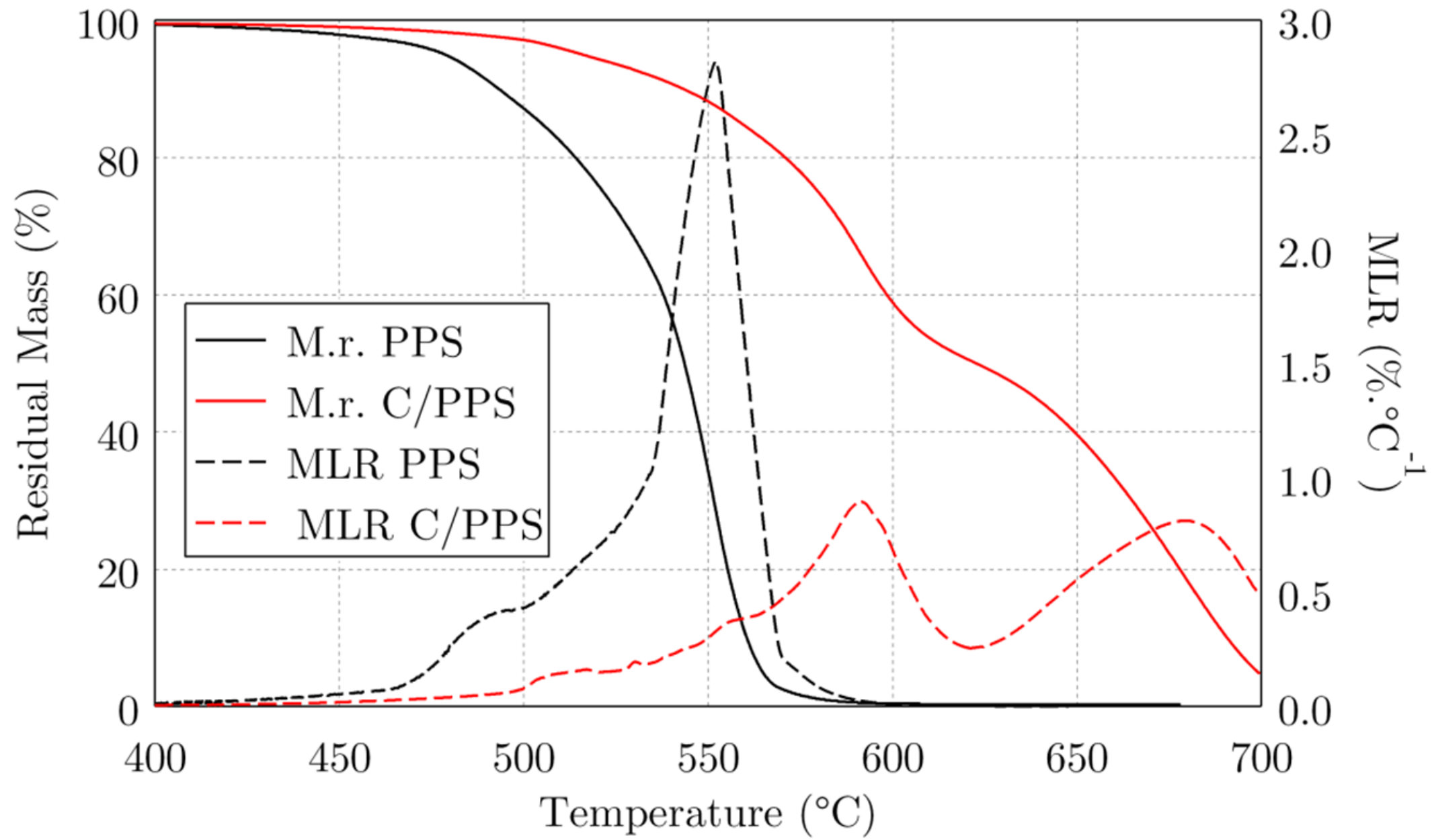
Residual Mass (%)
MLR (%.°C^{-1})
Temperature (°C)
M.r. PPS
M.r. C/PPS
MLR PPS
MLR C/PPS
100
80
60
40
20
0
3.0
2.5
2.0
1.5
1.0
0.5
0.0
400
450
500
550
600
650
700

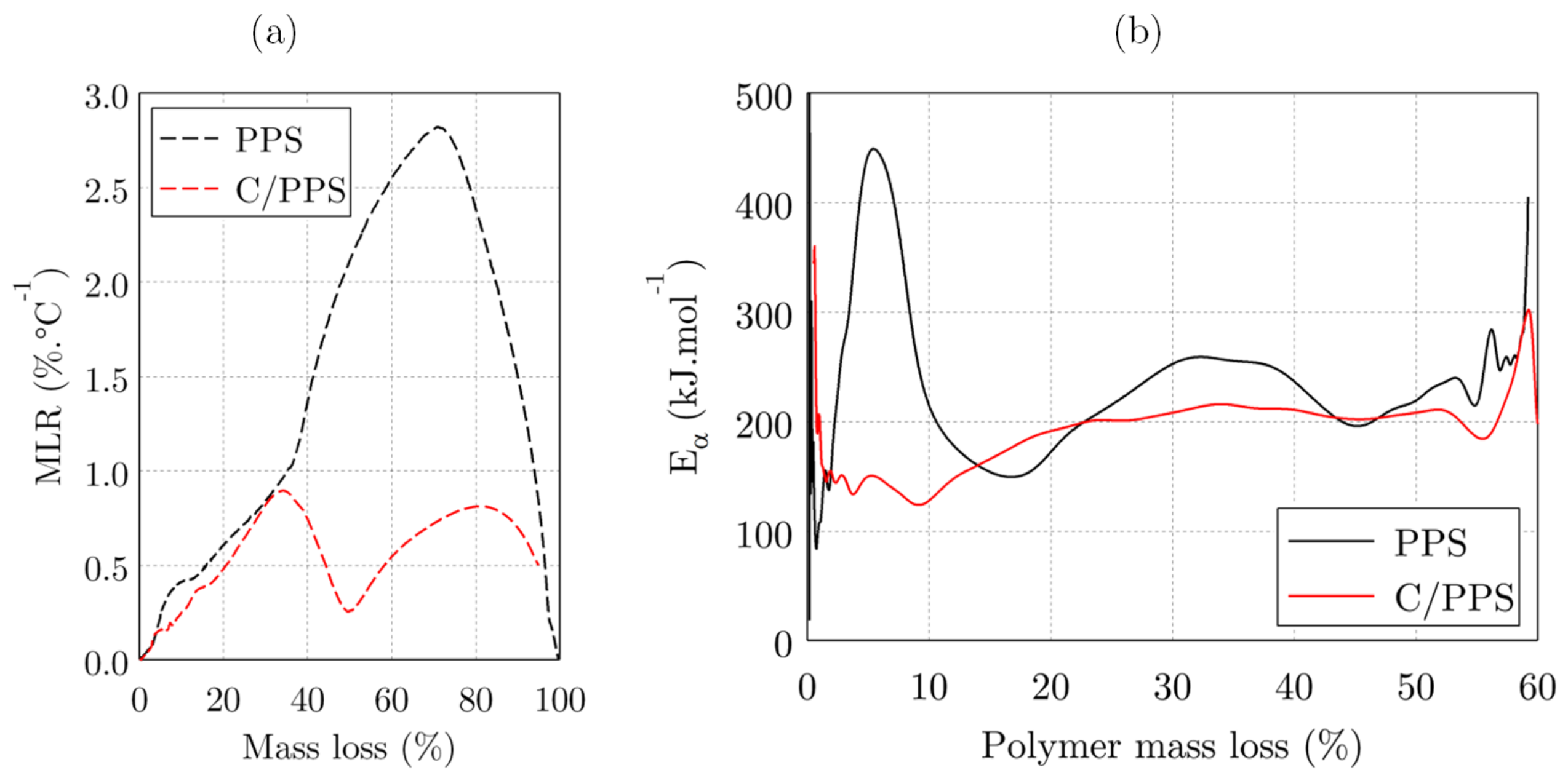
(a)
(b)
PPS
C/PPS
MLR (%.°C-1)
Mass loss (%)
Eα (kJ.mol-1)
Polymer mass loss (%)
0.0
0.5
1.0
1.5
2.0
2.5
3.0
0
20
40
60
80
100
0
100
200
300
400
500
0
10
20
30
40
50
60

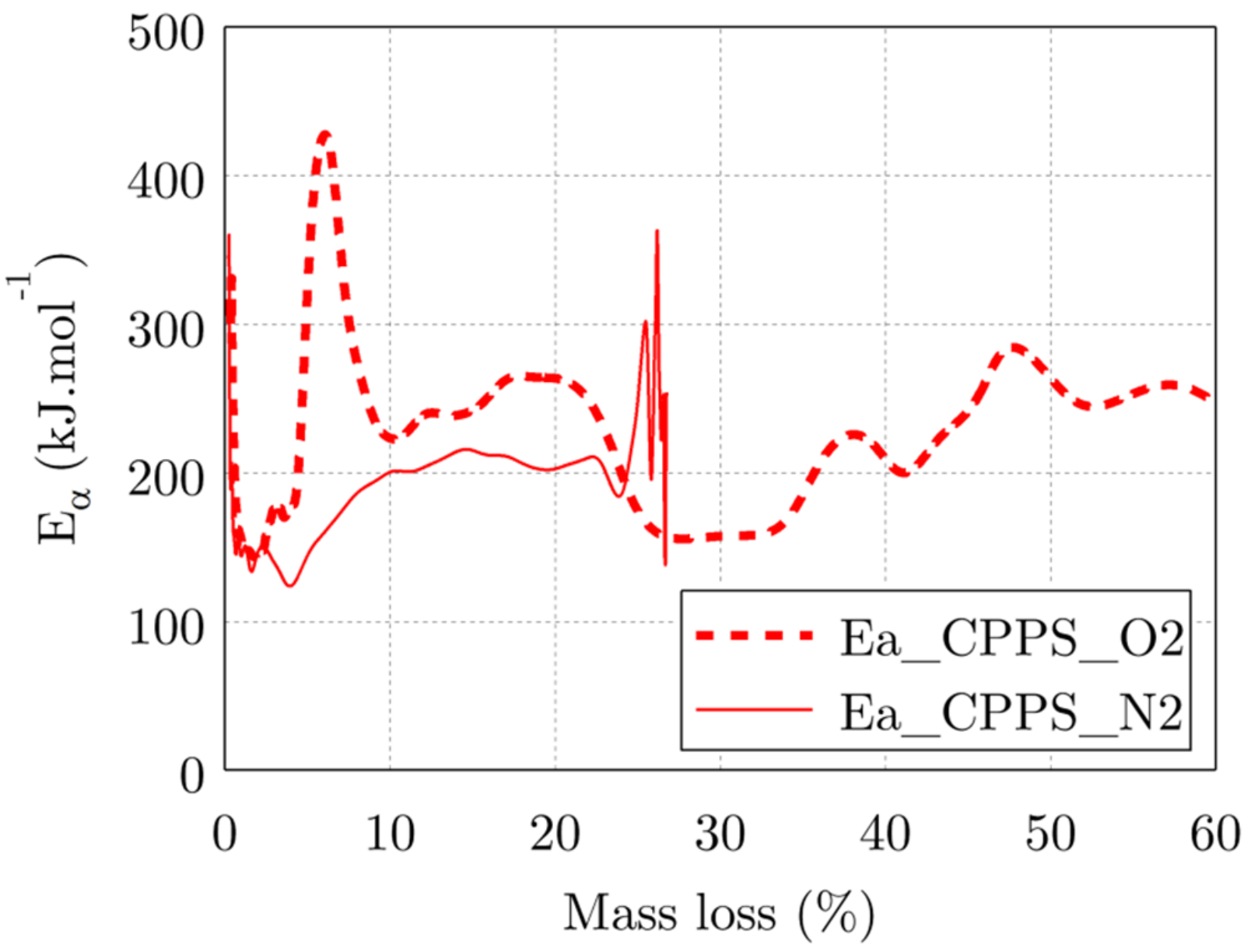
500
400
300
200
100
0
E_α (kJ.mol^{-1})
0
10
20
30
40
50
60
Mass loss (%)
Ea_CPPS_O2
Ea_CPPS_N2

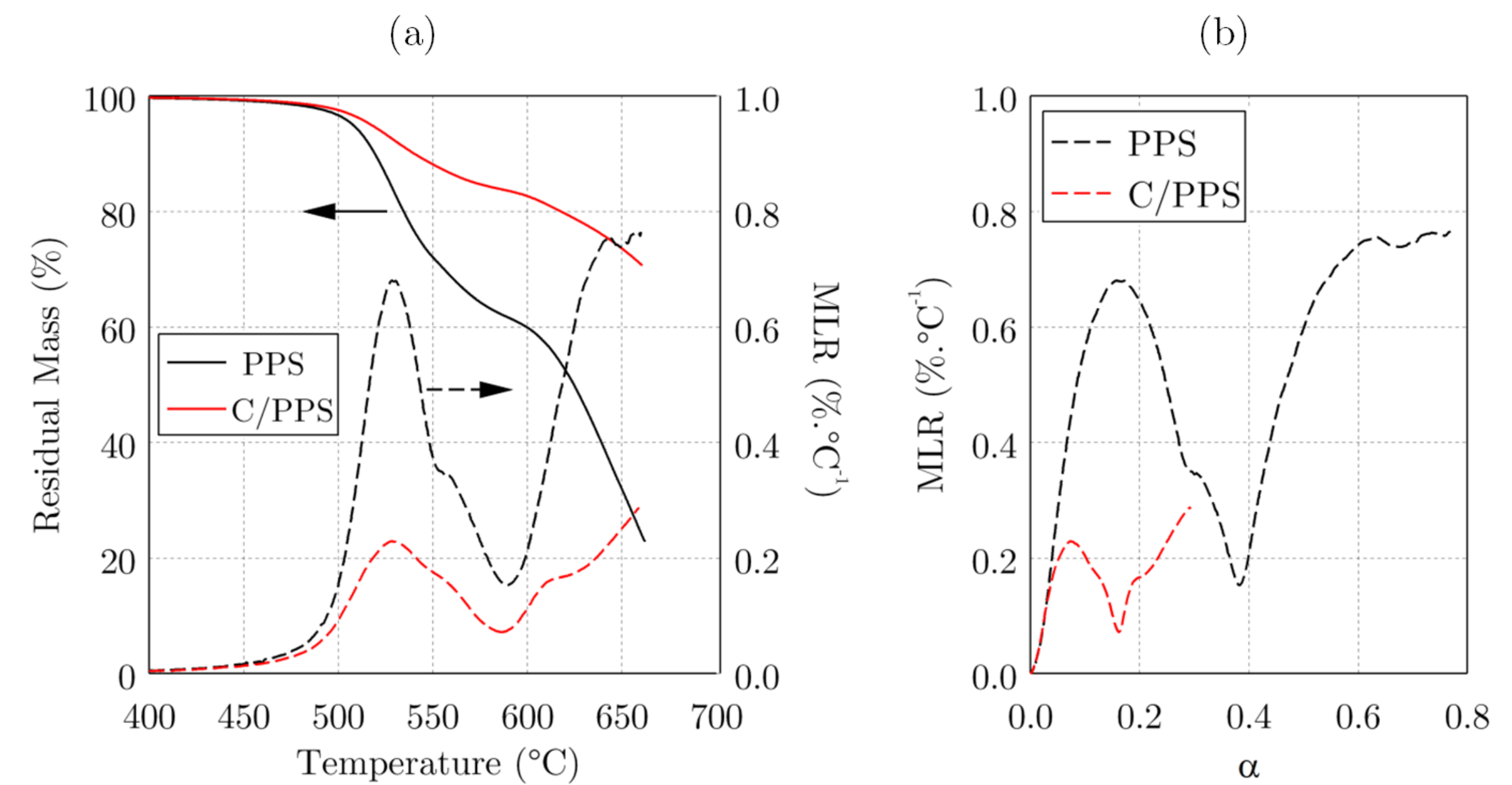
(a)
(b)
Residual Mass (%)
MLR (%.°C-1)
Temperature (°C)
PPS
C/PPS
MLR (%.°C-1)
α
0
20
40
60
80
100
0.0
0.2
0.4
0.6
0.8
1.0
400
450
500
550
600
650
700
0.0
0.2
0.4
0.6
0.8

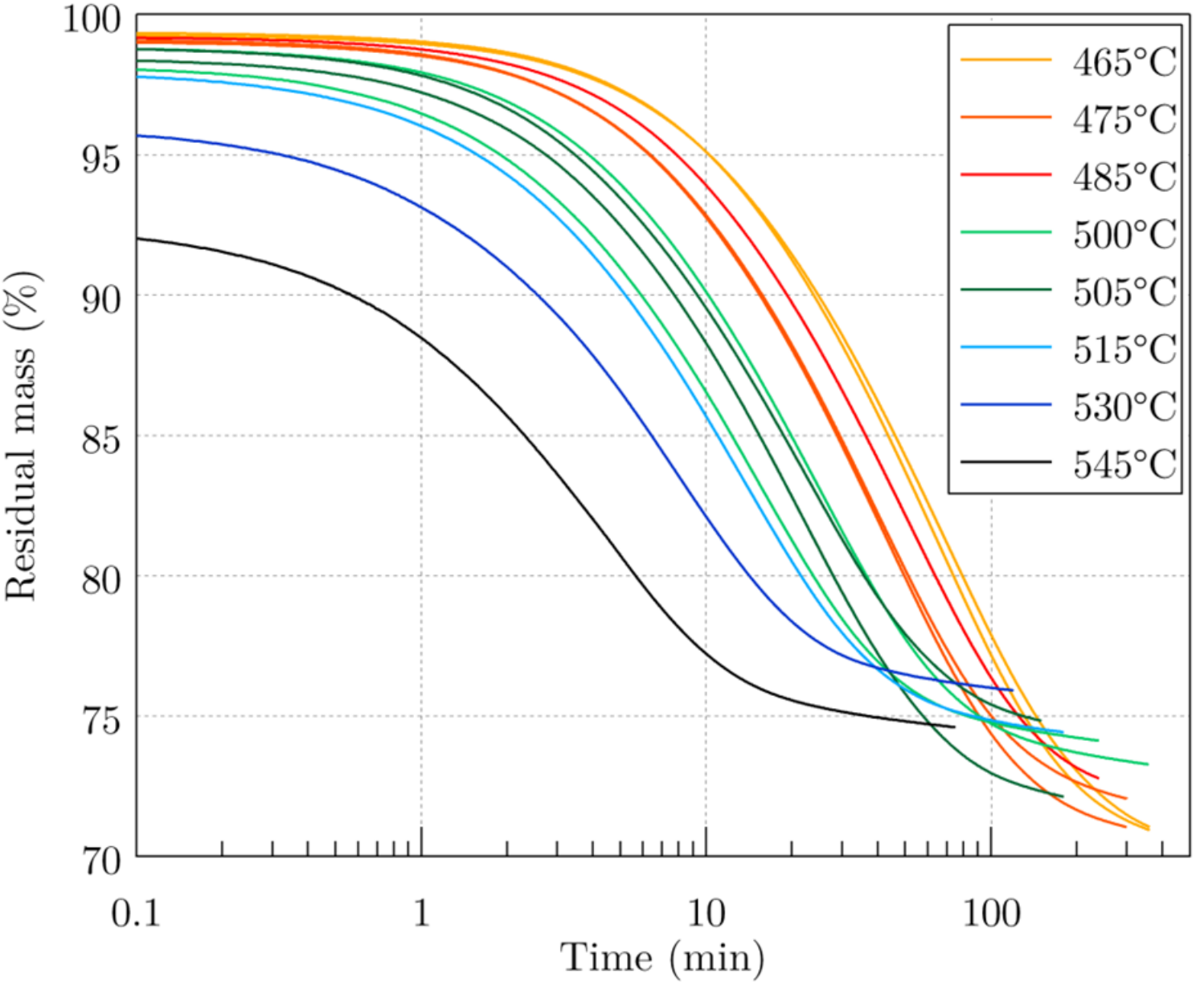
100
95
90
85
80
75
70
Residual mass (%)
0.1
1
10
100
Time (min)
465°C
475°C
485°C
500°C
505°C
515°C
530°C
545°C

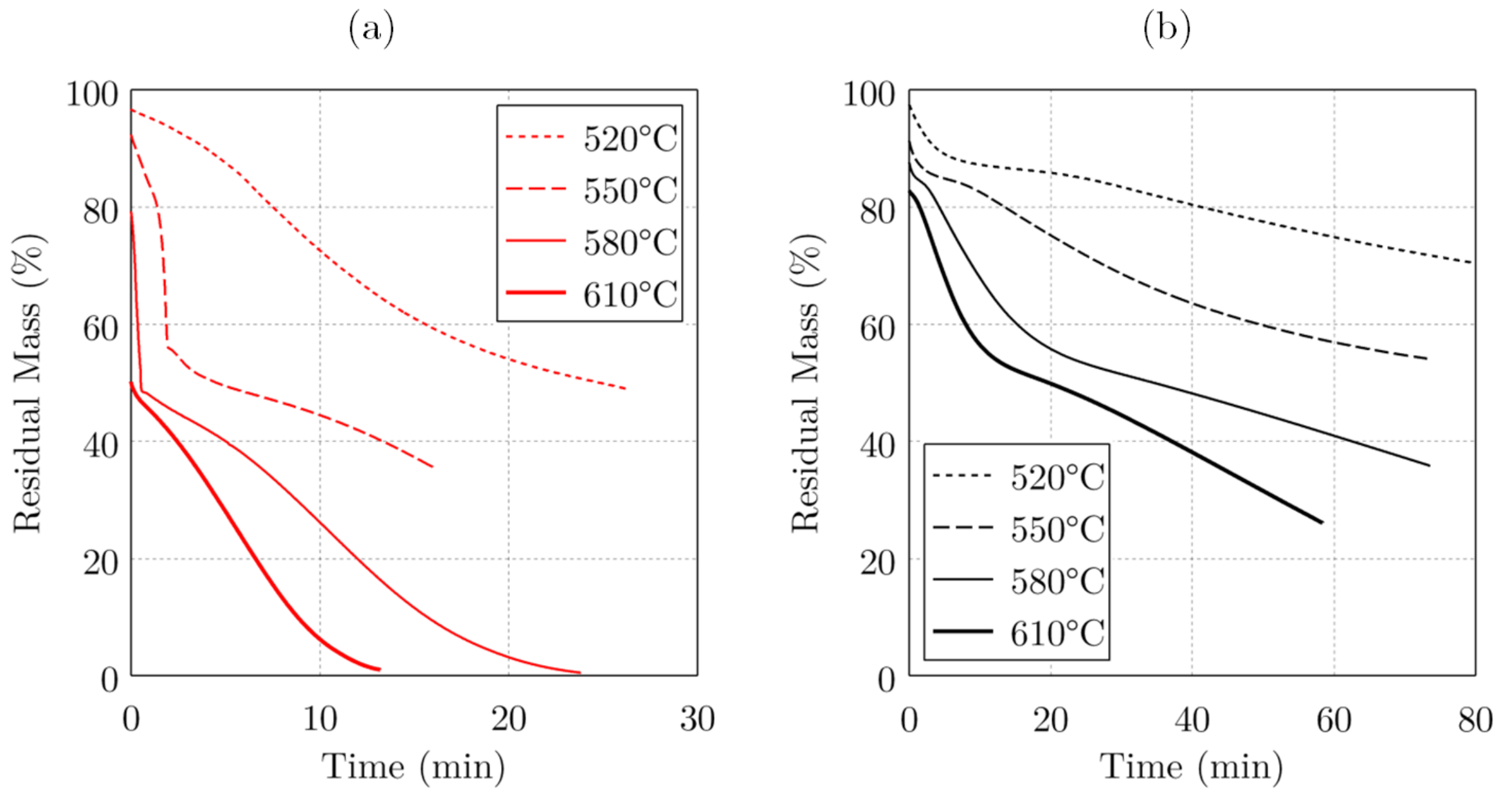
(a)
(b)
Residual Mass (%)
Time (min)
520°C
550°C
580°C
610°C
0
20
40
60
80
100
0
10
20
30

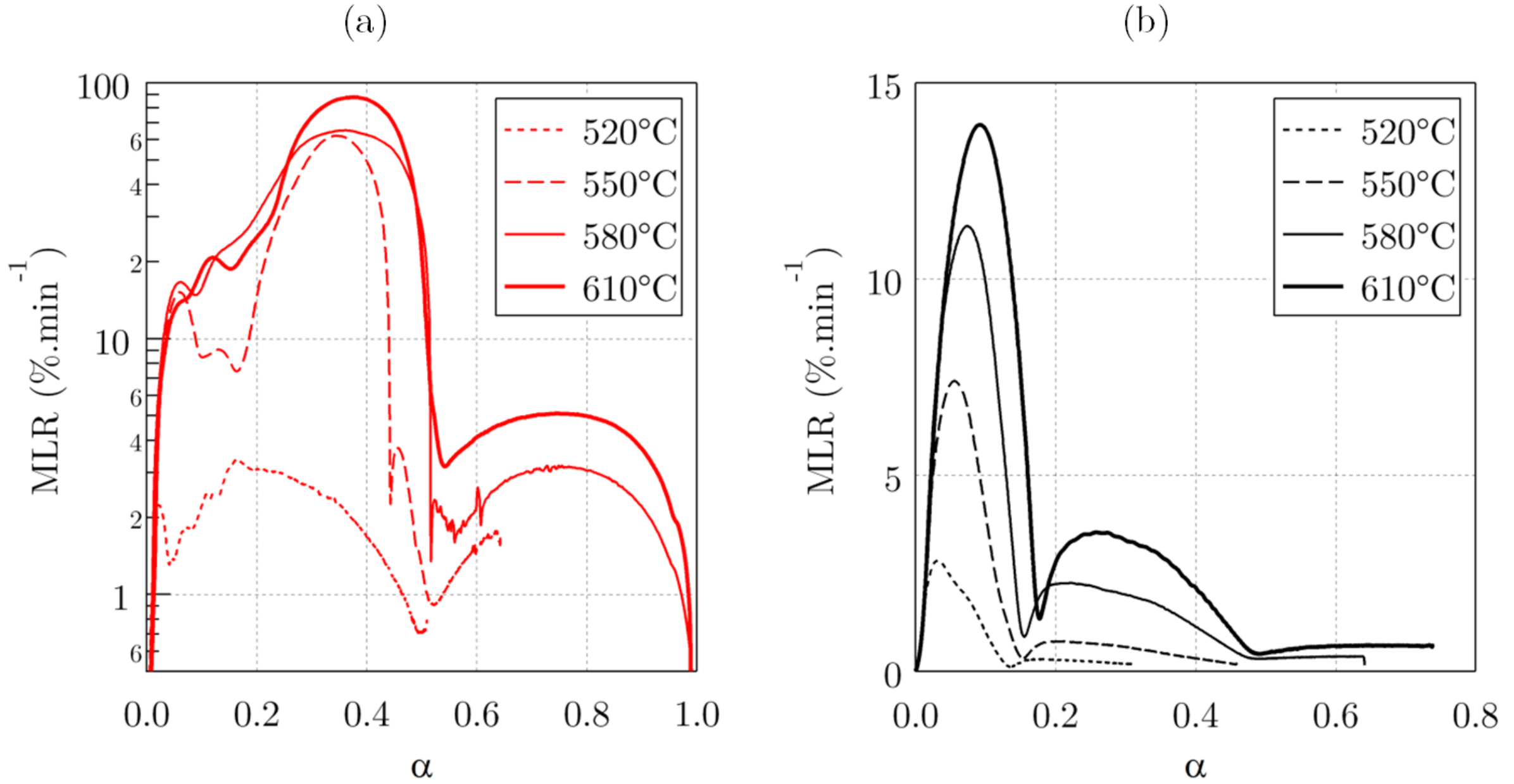
(a)
(b)
100
6
4
2
10
6
4
2
1
6
MLR (%.min-1)
520°C
550°C
580°C
610°C
0.0
0.2
0.4
0.6
0.8
1.0
α
15
10
5
0
MLR (%.min-1)
520°C
550°C
580°C
610°C
0.0
0.2
0.4
0.6
0.8
α

Tables

	N_2	O_2
Plain PPS resin	503°C	502°C
C/PPS composite	483°C	515°C

Table 1 - Temperature at the onset of decomposition of plain PPS and C/PPS composites at a heating rate 10°C/min

	N_2	O_2	Air
Plain PPS resin	523°C	530°C	508°C
C/PPS composite	525°C	526°C	517°C

Table 2 - Temperature at the onset of decomposition of plain PPS and C/PPS composites at a heating rate 20°C/min